

## Ca<sup>2+</sup>-induced activation of ATPase activity of myosin Va is accompanied with a large conformational change<sup>☆</sup>

Xiang-dong Li,<sup>a</sup> Katsuhide Mabuchi,<sup>b</sup> Reiko Ikebe,<sup>a</sup> and Mitsuo Ikebe<sup>a,\*</sup>

<sup>a</sup> Department of Physiology, University of Massachusetts Medical School, 55 Lake Avenue North, Worcester, MA 01655, USA

<sup>b</sup> Boston Biomedical Research Institute, Watertown, MA 02472, USA

Received 20 December 2003

### Abstract

We succeeded in expressing the recombinant full-length myosin Va (M5Full) and studied its regulation mechanism. The actin-activated ATPase activity of M5Full was significantly activated by Ca<sup>2+</sup>, whereas the truncated myosin Va without C-terminal globular domain is not regulated by Ca<sup>2+</sup> and constitutively active. Sedimentation analysis showed that the sedimentation coefficient of M5Full undergoes a Ca<sup>2+</sup>-induced conformational transition from 14S to 11S. Electron microscopy revealed that at low ionic strength, M5Full showed an extended conformation in high Ca<sup>2+</sup> while it formed a folded shape in the presence of EGTA, in which the tail domain was folded back towards the head–neck region. Furthermore, we found that the motor domain of myosin Va folds back to the neck domain in Ca<sup>2+</sup> while the head–neck domain is more extended in EGTA. It is thought that the association of the motor domain to the neck inhibits the binding of the tail to the neck thus destabilizing a folded conformation in Ca<sup>2+</sup>. This conformational transition is closely correlated to the actin-activated ATPase activity. These results suggest that the tail and neck domain play a role in the Ca<sup>2+</sup> dependent regulation of myosin Va.

© 2004 Elsevier Inc. All rights reserved.

Myosins are motor proteins that interact with actin filaments and convert energy from ATP hydrolysis into mechanical force. In addition to well-characterized conventional, filament forming myosin-II of muscle and non-muscle cells, a number of unconventional myosins have been discovered and it is known that myosin constitutes superfamily. The myosin superfamily is currently organized into 18 classes based upon phylogenetic sequence comparisons of the motor domain [1–4]. Among them, myosin Va is the best characterized unconventional myosin. However, it is still not clear the mechanism by which myosin Va works as a motor protein, especially how it is regulated.

Myosin Va was initially characterized as an unusual calmodulin binding protein from the brain with a number of myosin-like biochemical properties [5–7]. Myosin Va is especially abundant in neurons and con-

stitutes 0.2% of the total protein in the brain [8]. So far, myosin Va has been purified from chicken and mouse brain. The actin-activated ATPase activities of tissue-isolated myosin Va, both chicken brain myosin Va and mouse brain myosin Va, are well regulated by Ca<sup>2+</sup> [8,9]. On the other hand, Ca<sup>2+</sup> does not enhance the ATPase activity of expressed recombinant truncated myosin Va, such as myosin Va HMM and S1 [9–11].

Ca<sup>2+</sup> has strikingly different effects on ATPase activity and *in vitro* motility activity of myosin Va. Although Ca<sup>2+</sup> enhances the ATPase activity of tissue-isolated myosin Va, it suppresses *in vitro* motility of myosin Va [8]. It is puzzling that myosin Va has very low actin-activated ATPase activity in EGTA condition, yet it has good motility in similar conditions. Similar phenomena were found for expressed truncated myosin Va. Although the ATPase of recombinant truncated myosin Va is not regulated by Ca<sup>2+</sup>, its motility was inhibited by Ca<sup>2+</sup> [10,11]. The reason why tissue-isolated myosin Va and expressed myosin Va fragments show different properties is unknown. Obvious possibility is that the tail domain influences the Ca<sup>2+</sup> dependent regulation. Alternatively, the difference may be attributed to the

<sup>☆</sup> While we were preparing this paper, it appeared online that Wang et al. [32] found the formation of a folded structure of myosin Va at low ionic strength in EGTA but an extended structure in Ca<sup>2+</sup>.

\* Corresponding author. Fax: 1-508-856-4600.

E-mail address: [mitsuo.ikebe@umassmed.edu](mailto:mitsuo.ikebe@umassmed.edu) (M. Ikebe).

differences in the post-translational modifications of recombinant and tissue-isolated myosin Va or the sub-unit compositions and it is reported that tissue-isolated myosin Va contains dynein light chain [12].

In this paper, we succeeded in functionally expressing recombinant full-length myosin Va and studied  $\text{Ca}^{2+}$  dependent regulation of myosin Va by examining the expressed full-length myosin Va and various truncated variants. The results indicated that full-length myosin Va undergoes a  $\text{Ca}^{2+}$ -induced conformational change, which is closely correlated to the actin-activated ATPase activity. Myosin Va showed an extended conformation in  $\text{Ca}^{2+}$  while a folded conformation is favored in the absence of  $\text{Ca}^{2+}$  in physiological ionic conditions.

## Materials and methods

**Materials.** Restriction enzymes and modifying enzymes were purchased from New England Biolab (Beverly, MA). Actin was prepared from rabbit skeletal muscle acetone powder according to Spudich and Watt [13]. Recombinant calmodulin of *Xenopus* oocyte [14] was expressed in *Escherichia coli* as described [15].  $\text{Ni}^{2+}$ -NTA-agarose was purchased from Qiagen (Hilden, Germany). Anti-FLAG M2 antibody, anti-FLAG M2 affinity gel, FLAG peptide (Asp Tyr Lys Asp Asp Asp Asp Lys), phosphoenolpyruvate (PEP), 2,4-dinitrophenyl-hydrazine, and pyruvate kinase were from Sigma (St. Louis, MO).

**Construction of myosin Va expression vector.** A baculovirus transfer vector for mouse myosin Va (M5Full) in pFastBac (Invitrogen, CA) was produced as follows. A unique *SpeI* site was created at nucleotide 3316 of DHM5 [10]. A cDNA fragment 3316–5602 flanked by *SpeI* and *KpnI* sites was introduced to DHM5 to produce a full-length myosin Va construct. The nucleotides at the created *SpeI* site were changed to resume the authentic sequence. An N-terminal tag (MSYYH HHHHH DYKDD DDKNI PTEN LYFQG AMGIR NSKAY) containing a sequence of hexa-histidine-tag and FLAG-tag was added to the N-terminus of M5Full. For M5HMM, a stop codon was introduced at the nucleotide 3316. Vector containing nucleotide 1–2468 of myosin Va (M5IQ2) was prepared as described previously [10].

**Expression and purification of myosin Va.** To express recombinant M5Full, Sf9 cells (about  $1 \times 10^9$ ) were co-infected with two separate viruses expressing the myosin Va heavy chain and calmodulin, respectively. The infected cells were seeded in 15 large flasks (175 cm<sup>2</sup>) and cultured at 28 °C for 3 days. Cells were harvested and washed with 4 mM EGTA in TBS (50 mM Tris-HCl, pH 7.5, 0.15 M NaCl). Cell pellets were then lysed with sonication in 20 ml of lysis buffer [50 mM Tris-HCl, pH 7.5, 0.3 M NaCl, 1 mM EGTA, 0.02% NaN<sub>3</sub>, 5 mM ATP, 5 mM of 2-mercaptoethanol, 10 µg/ml leupeptin, 0.2 mg/ml trypsin inhibitor (egg), and 0.5% Triton X-100]. After centrifugation at 120,000g for 30 min, the supernatant was incubated with 1.0 ml anti-FLAG M2 affinity resin in a 50-ml conical tube on a rotating wheel in a cold room for 2 h. The resin suspension was then loaded on a column (1 × 10 cm) and washed with 30 ml solution-A (50 mM Tris-HCl, pH 7.5, 0.3 M NaCl, 0.2 mM EGTA, 2 µg/ml leupeptin, and 5 mM of 2-mercaptoethanol). Myosin Va, bound to anti-FLAG agarose, was eluted with 0.1 mM FLAG peptide in solution-A and concentrated by Vivaspin (Vivascience, Germany). The collected myosin Va was dialyzed overnight against 1 L buffer D [20 mM Mops (pH 7.0), 0.2 M NaCl, 0.1 mM EGTA, and 1 mM DTT].

A similar procedure was used for purification of M5HMM that has an N-terminal FLAG-tag. M5IQ2 was purified by  $\text{Ni}^{2+}$ -NTA-agarose affinity chromatography as described before [10], since this construct has C-terminal hexa-histidine-tag. Protein concentration was deter-

mined by Coomassie Brilliant Blue R250 staining of SDS-PAGE (7.5–20%) using smooth muscle myosin heavy chain as standard. The molecular weights of heavy chain were 220, 134, 96, and 220 kDa for M5Full, M5HMM, M5IQ2, and smooth muscle myosin, respectively, calculated from their amino acid composition. All concentrations of myosin Va in this paper are referred to the concentration of head.

**ATPase assay.** Since myosin Va ATPase activity, significantly inhibited by product, ADP, we used an ATP regeneration system to measure its activity. The MgATPase activity was measured at 25 °C in a solution containing 10–100 nM myosin Va, 20 mM Mops (pH 7.0), 1 mM MgCl<sub>2</sub>, 0.25 mg/ml BSA, 1 mM DTT, 2.5 mM PEP, 20 U/ml pyruvate kinase, 12 µM calmodulin, 100 mM KCl, 0.5 mM ATP, 1 mM EGTA-CaCl<sub>2</sub> buffer system, and various concentrations of actin. The reaction was stopped at various times between 4 and 60 min by adding 100 µl reaction solution to a 1.5-ml tube containing 350 µl of 0.36 mM of 2,4-dinitrophenyl hydrazine (Sigma, MO) and 0.4 M HCl. After incubation at 37 °C for 10 min, 250 µl of 2.5 M NaOH and 0.1 M EDTA was added to each tube and absorption at 460 nm was recorded. The standard curve was measured using 0–0.5 mM freshly prepared pyruvate solution.

**Analytical ultracentrifugation.** The myosin Va sample (about 1 ml) was dialyzed against 1 L buffer of 20 mM Mops (pH 7.0), 0.2 M NaCl, 0.1 mM EGTA, and 1 mM DTT. Just before running, MgCl<sub>2</sub> and EGTA concentration was adjusted to 1 mM for EGTA condition. For  $\text{Ca}^{2+}$  condition, MgCl<sub>2</sub> and CaCl<sub>2</sub> were adjusted to 1 mM, and EGTA was adjusted to 2.05, 1.41, 1.03, and 0.87 mM for pCa7, pCa6, pCa5, and pCa4 condition, respectively. For high salt condition, NaCl concentration was increased to 0.6 M by adding 5 M NaCl. The buffers for the reference were treated identically as samples. Sedimentation velocity was run at 42,000 rpm at 20 °C for 2 h in a Beckman Optima XL-I analytical ultracentrifuge. Sedimentation boundaries were analyzed using a time-derived sedimentation velocity program, i.e., DcDt [16] or DcDt plus [17]. The density and viscosity calculated with Sednterp for a solution containing 0.2 M NaCl and 1 mM MgCl<sub>2</sub> were 1.00658 g/ml and 1.0213 cp, respectively. Those values for a solution of 0.6 M NaCl and 1 mM MgCl<sub>2</sub> were 1.0228 g/ml and 1.0590 cp, respectively. The values of the partial specific volumes of M5Full (0.7323), M5HMM (0.7296), and M5IQ2 (0.7328) were calculated from the amino acid composition of heavy chain and calmodulin.

**Electron microscopy.** M5Full samples diluted to about 4 nM were absorbed onto a freshly cleaved mica surface for 30 s. Unbound proteins were rinsed away, and then the specimen was stabilized by brief exposure to uranyl acetate as described [18]. The specimen was visualized by the rotary shadowing technique according to Mabuchi [19] with a Philips 300 electron microscope at 60 kV.

## Results

### *Expression of recombinant full-length myosin Va and its fragments*

We succeeded in functionally expressing a full-length mouse myosin Va (M5Full). Myosin Va heavy chain was co-expressed with calmodulin light chain and purified as described in Materials and methods (Fig. 1). To eliminate any possible contamination of endogenous myosin of Sf9 cells, FLAG-tag was introduced to heavy chain. The expressed M5Full was composed of heavy chain with an apparent molecular weight of 190 kDa and calmodulin light chain and free from endogenous 200 kDa myosin II of Sf9 cells. There was no ATPase activity detected when non-infected Sf9 cell extract was

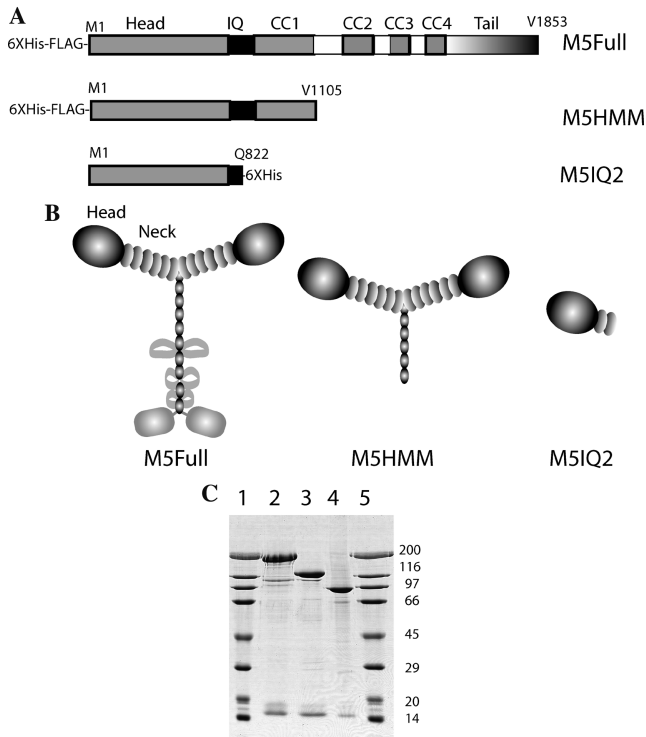


Fig. 1. Schematics of myosin Va constructs. (A) Schematic primary structure of myosin Va constructs expressed in this study. CC represents the coiled-coil sequence. IQ represents the calmodulin light chain binding domain. His-tag and FLAG-tag were added at N-terminus of M5Full and M5HMM, while His-tag was added at C-terminus of M5IQ2. (B) Schematic structure of myosin Va constructs based on its amino acid sequence and a schematic published previously [8]. The chain represents coiled-coil structure. (C) SDS-PAGE (7.5–20%) of purified M5Full (lane 2), M5HMM (lane 3), and M5IQ2 (lane 4). Lanes 1 and 5 are molecular weight markers with the molecular masses indicated on the right of lane 5 (in kDa).

subjected to anti-FLAG chromatography. Myosin Va HMM (M5HMM) containing the entire head, IQ domain, and coiled-coil domain and M5IQ2 containing entire head and 2 IQ domains were also isolated (Fig. 1C). These constructs were used for the experiments described in this study.

#### ATPase activity of recombinant myosin Va and its fragments

Fig. 2A shows the actin-activated ATPase activity of M5Full in the presence and absence of free  $\text{Ca}^{2+}$ . The actin-activated ATPase activity of M5Full showed strong  $\text{Ca}^{2+}$  dependence and the activity was increased approximately 9-fold in the presence of  $100\ \mu\text{M}$  free  $\text{Ca}^{2+}$  (Fig. 2A and Table 1). The result of M5Full is similar to that of tissue-isolated myosin Va [9,20]. On the other hand,  $\text{Ca}^{2+}$  increased the activity of M5HMM with much reduced extent than that of M5Full in the presence of  $12\ \mu\text{M}$  calmodulin (Fig. 2B). In the absence of exogenous calmodulin, actin-activated ATPase ac-

tivity of M5HMM was decreased at high  $\text{Ca}^{2+}$  as was reported previously [10], and it is thought that the decrease in the ATPase activity is due to the dissociation of calmodulin light chain. The ATPase activity of M5IQ2 showed reverse  $\text{Ca}^{2+}$  dependence and the activity was slightly higher in EGTA than in  $\text{Ca}^{2+}$  (Fig. 2C). Both truncated constructs have high ATPase activity in EGTA condition, which is similar to that of M5Full in  $\text{Ca}^{2+}$  condition. The results suggest that the  $\text{Ca}^{2+}$  dependent regulation observed for M5Full is due to the inhibition in EGTA rather than the activation in  $\text{Ca}^{2+}$ . Fig. 2D shows free  $\text{Ca}^{2+}$  concentration dependence of the actin-activated ATPase activity of M5Full. The activity was increased at higher than pCa5, suggesting that  $\text{Ca}^{2+}$  binding to calmodulin light chain is responsible for the activation. The result of M5Full is similar to that of tissue-isolated myosin Va and suggests that the tail domain of myosin Va is responsible for  $\text{Ca}^{2+}$  dependent regulation.

Fig. 3 shows KCl dependence of the actin-activated ATPase activity of M5Full. Interestingly,  $\text{Ca}^{2+}$  dependence was abolished at high ionic strength. The activity in  $\text{Ca}^{2+}$  condition was significantly increased at low ionic strength while the activity in EGTA was not strongly increased at low ionic strength. On the other hand, the activity of M5HMM was increased at low ionic strength for both  $\text{Ca}^{2+}$  and EGTA conditions. At low ionic strength, the activity ratio between M5Full and M5HMM markedly increased by  $\text{Ca}^{2+}$ , while at high ionic strength the activity ratio did not dramatically change by  $\text{Ca}^{2+}$  (Table 2). These results suggest that the activity of M5Full is inhibited at low  $\text{Ca}^{2+}$  and the inhibition is only achieved at low ionic strength.

#### $\text{Ca}^{2+}$ dependent conformational change of myosin Va

To understand the mechanism, by which  $\text{Ca}^{2+}$  changes the ATPase activity of M5Full, we studied the conformational changes of myosin Va constructs. First, we analyzed the sedimentation coefficient ( $S_{20,w}$ ) of myosin Va in EGTA and  $\text{Ca}^{2+}$  conditions by velocity sedimentation analysis. Purified myosin Va constructs in EGTA or pCa5 condition were subjected to analytical centrifugation. The apparent  $S_{20,w}$  of M5Full decreased significantly from 13.9S in EGTA to 11.3S in pCa5 condition (Fig. 4 and Table 3). Remarkably, the stimulation of actin-activated ATPase activity of M5Full by  $\text{Ca}^{2+}$  is accompanied with the decrease of  $S_{20,w}$  (Fig. 2D and Table 3). The coiled-coil structure of myosin Va is stable and it is unlikely that the two-headed structure of myosin Va is broken at high  $\text{Ca}^{2+}$ . Supporting this notion, M5HMM, containing partial coiled-coil domain, failed to show a decrease of  $S_{20,w}$ . Therefore, the results suggest that the observed change in the  $S_{20,w}$  of M5Full is due to the large change in the conformation. It is predicted that M5Full forms a more compact conformation in the presence of low  $\text{Ca}^{2+}$  than in high  $\text{Ca}^{2+}$ .

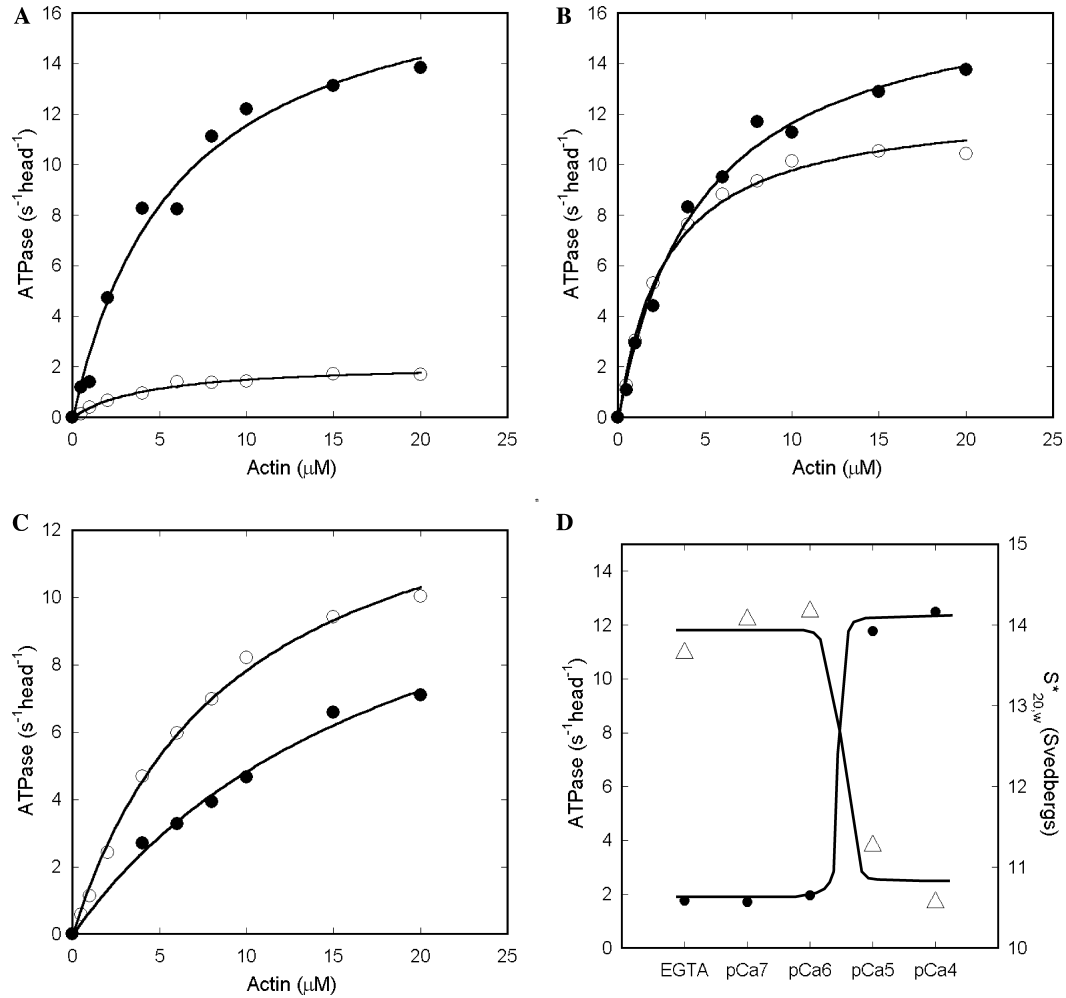


Fig. 2. MgATPase activity of myosin Va constructs. (A–C) The actin dependence of ATPase activity of M5Full (A), M5HMM (B), and M5IQ2 (C) in EGTA (open circle) and pCa4 condition (closed circle). The solid lines in (A–C) are fit to the Michaelis–Menten equation. The fitting data are summarized in Table 1. Assay conditions were described in Materials and methods. (D) Effects of Ca<sup>2+</sup> on the ATPase activity (closed circle) and sedimentation coefficient (open triangular) of M5Full. The ATPase activity was measured at 25 °C in a solution of 20 mM Mops (pH 7.0), 0.1 M KCl, 1 mM MgCl<sub>2</sub>, 1 mM DTT, 0.25 mg/ml BSA, 12 μM calmodulin, 20 μM actin, 0.5 mM ATP, 2.5 mM PEP, and 20 U/ml pyruvate kinase. EGTA (1 mM) was added for EGTA condition, whereas 1 mM CaCl<sub>2</sub> and various concentrations of EGTA were added for pCa7–pCa4 conditions as described in Materials and methods. Sedimentation coefficient was measured as described in Materials and methods.

Table 1  
V<sub>max</sub> and K<sub>actin</sub> of actin-activated ATPase activity of myosin Va

	EGTA condition			Ca <sup>2+</sup> condition		
	V <sub>0</sub> (s <sup>-1</sup> head <sup>-1</sup> )	V <sub>max</sub> (s <sup>-1</sup> head <sup>-1</sup> )	K <sub>actin</sub> (μM)	V <sub>0</sub> (s <sup>-1</sup> head <sup>-1</sup> )	V <sub>max</sub> (s <sup>-1</sup> head <sup>-1</sup> )	K <sub>actin</sub> (μM)
M5Full	0.05	2.15	4.38	0.06	18.52	6.02
M5HMM	0.09	12.48	2.75	0.09	17.30	4.84
M5IQ2	0.07	15.07	9.21	0.07	14.45	19.87

Assay conditions were as described in the legend to Fig. 1. Basal activity (V<sub>0</sub>) was deducted. Curves are the least squares fits of the data points based upon the equation:  $V = (V_{max} * [actin]) / (K_{actin} + [actin])$ .

On the other hand, the S<sub>20,w</sub> of M5Full at high ionic strength slightly increased from 9.4 in EGTA to 9.7 in pCa5 (Table 2). Same results were obtained with several independent preparations. Both values were similar to that in Ca<sup>2+</sup> at low ionic strength, suggesting that the formation of a compact structure is abolished at high ionic strength. In contrast to M5Full, the S<sub>20,w</sub> for

M5HMM rather increased from 8.7S in EGTA to 9.5S in Ca<sup>2+</sup> condition (Fig. 4 and Table 3). Ca<sup>2+</sup> induced the slight decrease of S<sub>20,w</sub> with M5IQ2 (Fig. 4 and Table 3). While the change was small, the same results were obtained repeatedly, therefore, the change in S<sub>20,w</sub> of M5IQ2 may reflect the Ca<sup>2+</sup>-induced release of the bound calmodulin [10].

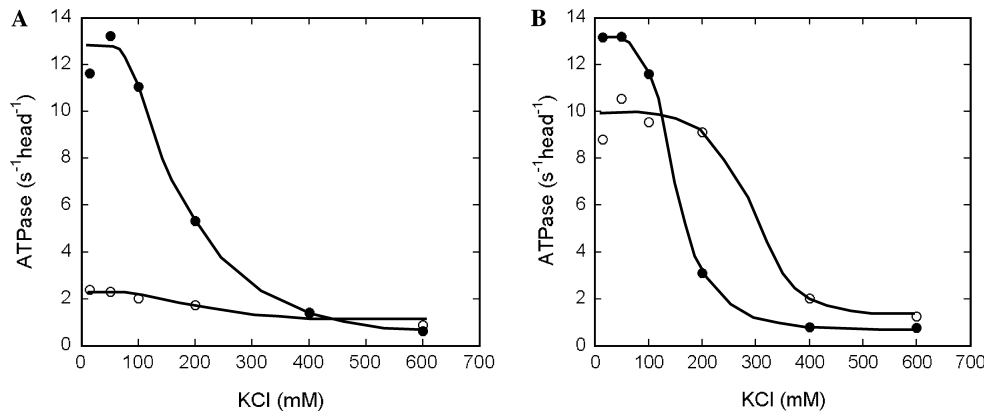


Fig. 3. Effects of KCl on the ATPase activity of M5Full (A) and M5HMM (B). The assay was carried in a solution containing 20 mM Mops (pH 7.0), 1 mM MgCl<sub>2</sub>, 1 mM DTT, 0.25 mg/ml BSA, 12 μM calmodulin, 20 μM actin, 0.5 mM ATP, 2.5 mM PEP, 20 U/ml pyruvate kinase, 20 μM actin, and various concentrations of KCl at 25 °C. One millimolar EGTA (open circle) and pCa5 (closed circle).

Table 2

Comparison of M5Full ATPase and M5HMM ATPase at low salt and high salt conditions

	KCl (mM)	M5Full (s <sup>-1</sup> head <sup>-1</sup> )	M5HMM (s <sup>-1</sup> head <sup>-1</sup> )	Ratio
EGTA	100	2.02	9.55	0.21
	600	0.88	1.25	0.70
pCa5	100	11.07	11.61	0.95
	600	0.64	0.77	0.83

Assay conditions were as described in the legend to Fig. 3. Ratio is calculated by dividing M5Full ATPase activity with M5HMM ATPase activity in same conditions.

To visualize the nature of the conformational change of M5Full, we examined the structure of M5Full by rotary shadowing of electron microscopy. Fig. 5 shows the representative images of M5Full in various conditions. At high ionic strength at low Ca<sup>2+</sup>, M5Full showed an extended conformation that was similar to those images previously reported [8]. On the other hand, we found a folded shape of M5Full at low ionic strength in the presence of EGTA, in which the tail domain was folded back towards the head–neck region. In the Ca<sup>2+</sup> condition, we predominantly found an extended conformation even at low ionic strength. These results are consistent with centrifugation analysis and show that 14S M5Full represents a folded conformation, while 11S M5Full represents an extended conformation. Furthermore, we found that the head of myosin Va appears large and globular with no obvious neck domain in high Ca<sup>2+</sup> regardless of ionic strength. On the other hand, in low Ca<sup>2+</sup> myosin Va showed smaller globular head connected with long neck domain (Fig. 5).

## Discussion

We found that myosin Va (M5Full) exhibits a Ca<sup>2+</sup> dependent large change in the S<sub>20,w</sub> at physiological ionic strength. It is known that S<sub>20,w</sub> is related to the molecular

weight. Theoretically, for random coils like large DNA molecules, S<sub>20,w</sub> is proportional to M<sup>1/2</sup>, whereas, for spherical molecules, S<sub>20,w</sub> is proportional to M<sup>2/3</sup>. It was reported that Ca<sup>2+</sup> induces the dissociation of calmodulin from myosin Va [10,20]. The number of dissociated calmodulin ranges from 1 to 1.3 [20] to 2 [10] from each heavy chain. If we assume that 4 of 12 bound calmodulin dissociated from myosin Va in Ca<sup>2+</sup> condition, the molecular weight of myosin Va will decrease from 644 kDa in EGTA condition to 576 kDa in Ca<sup>2+</sup> condition. The anticipated decrease in S<sub>20,w</sub> value is from 13.9S in EGTA condition to 13.1 (linear shape) or 12.9 (spherical shape). Both calculated numbers are much larger than the observed S<sub>20,w</sub> in Ca<sup>2+</sup> condition, so the decrease of S<sub>20,w</sub> is not due to the dissociation of calmodulin, but to conformational change. Based upon rotary shadowing of electron microscopy, it was found that M5Full forms a folded conformation at low Ca<sup>2+</sup> and low ionic strength. In this conformation, myosin Va tail bent back to the head–neck region of the molecule. On the other hand, M5Full forms a more extended conformation at high Ca<sup>2+</sup>. At high ionic strength, an extended conformation dominates over a folded conformation regardless of the Ca<sup>2+</sup> concentration that is reflected by the decrease in S<sub>20,w</sub>. Ca<sup>2+</sup> concentration required for the shift in conformation is pCa6–pCa5 based upon the change in the S<sub>20,w</sub>. This suggests that the conformational change is initiated by the binding of Ca<sup>2+</sup> to calmodulin light chain that is associated at the neck of myosin Va. It should be mentioned that myosin Va showed several apparently different shapes in low Ca<sup>2+</sup> at low ionic strength, although the molecules showed compact structures. This suggests that the attachment of the tail domain to the neck domain is not tight and there is enough flexibility to allow myosin Va molecules to take various conformations.

We also found that Ca<sup>2+</sup> changes the head–neck conformation regardless of the ionic strength. At high Ca<sup>2+</sup>, the characteristic long neck domain of myosin Va is not evident and two large globular heads are observed.

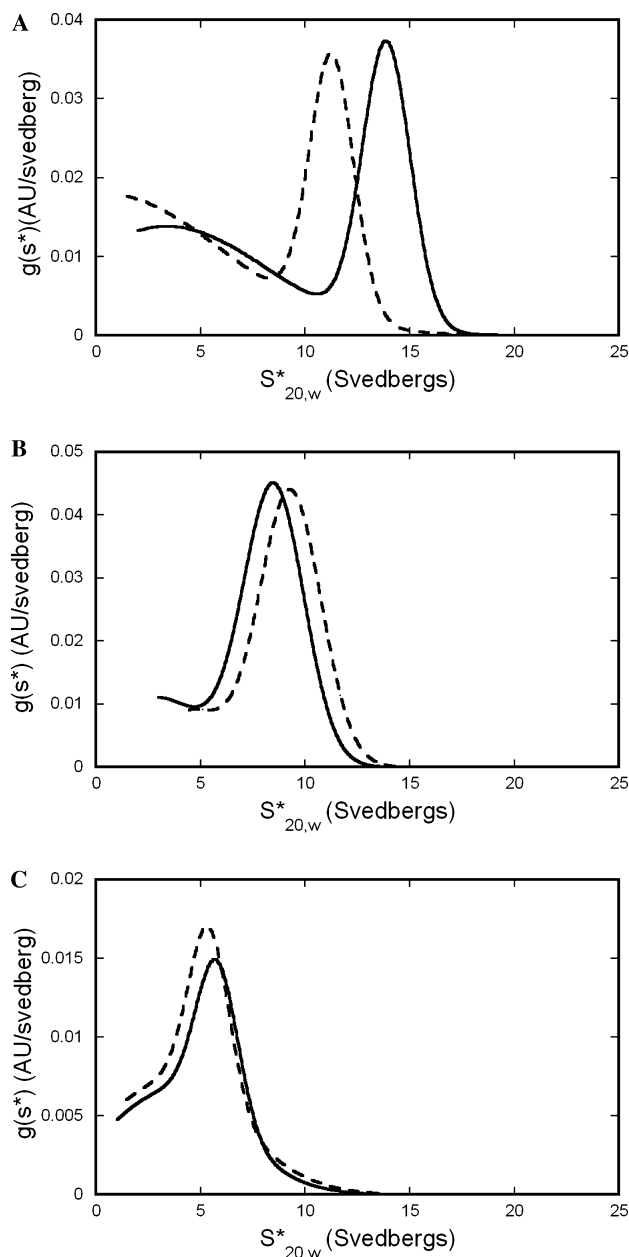


Fig. 4. Apparent sedimentation coefficient distributions for myosin Va constructs. Sedimentation velocity was determined in solutions containing 20 mM Mops (pH 7.0), 0.2 M NaCl, 1 mM DTT, and 1 mM EGTA (solid line). EGTA was replaced by EGTA–CaCl<sub>2</sub> buffer for pCa5 condition (broken line). The velocity runs were carried out at 42,000 rpm at 20 °C for M5Full (A), M5HMM (B), and M5IQ2 (C). The x-axis,  $S^*_{20,w}$ , is the apparent sedimentation coefficient.

We think that the globular motor domain of myosin Va is folded back to the neck domain at high Ca<sup>2+</sup> to create an apparently large globular head (Fig. 5). At low ionic strength, the attachment of the motor domain to the neck domain in Ca<sup>2+</sup> may prevent the interaction of the tail domain at the neck domain thus inhibiting the formation of a folded conformation. The Ca<sup>2+</sup>-induced increase in  $S_{20,w}$  with M5Full in high salt (9.4S–9.7S) and M5HMM

Table 3  
Sedimentation coefficient ( $S_{20,w}$ ) of myosin Va constructs

	EGTA	pCa7	pCa6	pCa5	pCa4
M5Full <sup>a</sup>	13.9	14.1	14.2	11.3	10.6
M5Full <sup>b</sup>	9.4	\	\	9.7	\
M5HMM <sup>a</sup>	8.7	\	\	9.5	\
M5IQ2 <sup>a</sup>	5.8	\	\	5.4	\

<sup>a</sup> Analytical centrifugation was run in a solution of 20 mM Mops (pH 7.0), 0.2 M NaCl, 1 mM MgCl<sub>2</sub>, 1 mM DTT, and various concentration of EGTA and CaCl<sub>2</sub> as described in Materials and methods.

<sup>b</sup> Same condition as <sup>a</sup> except 0.6 M NaCl was used.

(8.7S–9.5S) supports the model (Fig. 5B) in which the head folds back to neck in high Ca<sup>2+</sup>.

Interestingly, the change in the conformation of M5Full was closely correlated with the change in the actin-activated ATPase activity. At low ionic strength, Ca<sup>2+</sup> markedly increases the actin-activated ATPase activity and this is accompanied by the change in the conformation from a folded to an extended. On the other hand, there was no change in the ATPase activity by Ca<sup>2+</sup> at high ionic strength, where the compact folded structure of myosin Va is not found. A similar relationship between the conformational change and ATPase activity of myosin has been known for vertebrate smooth muscle and non-muscle myosin II [21–25]. Vertebrate myosin II forms a folded conformation at low ionic strength in which the tail bent back towards the head–neck junction while it forms an extended conformation. A folded myosin II has a low ATPase activity while an extended myosin II shows significantly higher ATPase activity [21,24]. The change in the conformation of myosin II is regulated by regulatory light chain phosphorylation [23,24,26] and it is thought that the phosphorylation of the light chain induces the conformational change at the neck region where the light chain associates and this stabilizes the association of the tail domain to form a folded conformation. For myosin Va, it is anticipated that Ca<sup>2+</sup> binding to calmodulin light chain induces the conformational change of calmodulin at the neck domain, which destabilizes the association of the tail domain to the head–neck region of myosin Va.

Recently, a similar tail inhibition model was proposed for the regulation of kinesin, i.e., kinesin is in a folded conformation such that the kinesin globular tail domain interacts with and inhibits the kinesin motor activity [27]. Full-length kinesin undergoes a 9S–6S conformational transition, i.e., compact to extended conformation, whereas, C-terminal domain truncated kinesin constitutively in extended form [28]. Correspondingly, the ATPase activity of full-length kinesin is activated by cargo binding, whereas C-terminal domain truncated kinesin is constitutively active. Furthermore, it was found that the expressed C-terminal globular domain inhibits the ATPase activity of C-terminal domain truncated kinesin [29]. The present study suggests that there is a similarity in the regulatory mechanism between kinesin and myosin Va.

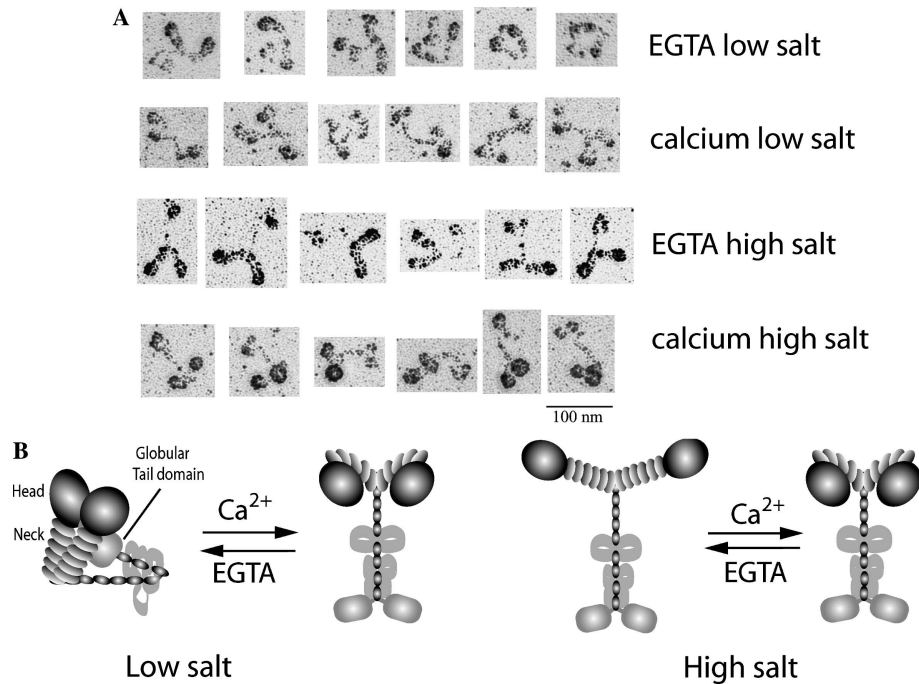


Fig. 5. Electron micrographs of M5Full and model for the regulation of M5Full. (A) Electron microscopic images of M5Full in various conditions. M5Full samples diluted to about 4 nM by dilution buffer were absorbed onto a freshly cleaved mica surface for 30 s. Unbound proteins were rinsed away, and then the specimen was stabilized by brief exposure to uranyl acetate as described under Materials and methods. Dilution buffers were as follows. EGTA-low salt, 1 mM MgCl<sub>2</sub>, 30% glycerol, 1 mM EGTA, and 50 mM ammonia acetate (pH 7.0); Ca<sup>2+</sup>-low salt, 1 mM MgCl<sub>2</sub>, 30% glycerol, 0.1 mM CaCl<sub>2</sub>, and 50 mM ammonia acetate (pH 7.0); EGTA-high salt, 1 mM MgCl<sub>2</sub>, 30% glycerol, 1 mM EGTA, and 600 mM ammonia acetate (pH 7.0); Ca<sup>2+</sup>-high salt, 1 mM MgCl<sub>2</sub>, 30% glycerol, 0.1 mM CaCl<sub>2</sub>, and 600 mM ammonia acetate (pH 7.0). (B) Schematic model of M5Full conformations. The motor domain is folded back to associate the neck domain in high Ca<sup>2+</sup>. At low salt condition, the tail globular domain interacts with the head–neck region to produce a compact structure in low Ca<sup>2+</sup>. This is inhibited in high Ca<sup>2+</sup> because the binding of the motor domain to the neck domain interferes with the association between the tail and the head–neck of myosin Va.

It is puzzling that the actin gliding activity of M5Full is active in EGTA where the ATPase activity is markedly inhibited. It is known that myosin Va is a processive motor with the step size of 36 nm/ATP hydrolysis [30]. Therefore, it can be calculated that ATPase cycle rate of 2 s<sup>-1</sup> in EGTA condition yields the actin gliding velocity of 0.07 μm/s, which is much slower than the observed actin gliding velocity in EGTA (0.3–0.5 μm/s) on glass surface [8,31]. One possibility to account for this discrepancy is that the attachment of myosin Va at the tail domain to glass surface diminishes the interaction between the tail and the head–neck domain releasing the inhibition. It is plausible, therefore, that the binding of tail domain to partner molecules may release the inhibition of the ATPase thus regulating myosin Va motor function. It requires further study to see whether cargo binding at the tail domain can activate myosin Va motor function.

### Acknowledgments

We thank the expert technical assistance of the lab members of Dr. Craig Peterson laboratory, especially, Kimberley Crowley, who ran most of analytical ultracentrifugations. This work was supported by NIH Grants AR1653 and GM55834.

### References

- [1] S.L. Reck-Peterson, D.W. Provance Jr., M.S. Mooseker, J.A. Mercer, Class V myosins, *Biochim. Biophys. Acta* 1496 (2000) 36–51.
- [2] V. Mermall, P.L. Post, M.S. Mooseker, Unconventional myosins in cell movement, membrane traffic, and signal transduction, *Science* 279 (1998) 527–533.
- [3] J.R. Sellers, Myosins: a diverse superfamily, *Biochim. Biophys. Acta* 1496 (2000) 3–22.
- [4] J.S. Berg, B.C. Powell, R.E. Cheney, A millennial myosin census, *Mol. Biol. Cell* 12 (2001) 780–794.
- [5] R.E. Larson, D.E. Pitta, J.A. Ferro, A novel 190 kDa calmodulin-binding protein associated with brain actomyosin, *Braz. J. Med. Biol. Res.* 21 (1988) 213–217.
- [6] R.E. Larson, F.S. Espindola, E.M. Espreafico, Calmodulin-binding proteins and calcium/calmodulin-regulated enzyme activities associated with brain actomyosin, *J. Neurochem.* 54 (1990) 1288–1294.
- [7] F.S. Espindola, E.M. Espreafico, M.V. Coelho, A.R. Martins, F.R. Costa, M.S. Mooseker, R.E. Larson, Biochemical and immunological characterization of p190-calmodulin complex from vertebrate brain: a novel calmodulin-binding myosin, *J. Cell Biol.* 118 (1992) 359–368.
- [8] R.E. Cheney, M.K. O’Shea, J.E. Heuser, M.V. Coelho, J.S. Wolenski, E.M. Espreafico, P. Forscher, R.E. Larson, M.S. Mooseker, Brain myosin-V is a two-headed unconventional myosin with motor activity [comment], *Cell* 75 (1993) 13–23.

- [9] F. Wang, L. Chen, O. Arcucci, E.V. Harvey, B. Bowers, Y. Xu, J.A. Hammer 3rd, J.R. Sellers, Effect of ADP and ionic strength on the kinetic and motile properties of recombinant mouse myosin V, *J. Biol. Chem.* 275 (2000) 4329–4335.
- [10] K. Homma, J. Saito, R. Ikebe, M. Ikebe, Ca<sup>2+</sup>-dependent regulation of the motor activity of myosin V, *J. Biol. Chem.* 275 (2000) 34766–34771.
- [11] K.M. Trybus, E. Kremntsova, Y. Freyzon, Kinetic characterization of a monomeric unconventional myosin V construct, *J. Biol. Chem.* 274 (1999) 27448–27456.
- [12] F.S. Espindola, D.M. Suter, L.B. Partata, T. Cao, J.S. Wolenski, R.E. Cheney, S.M. King, M.S. Mooseker, The light chain composition of chicken brain myosin-Va: calmodulin, myosin-II essential light chains, and 8-kDa dynein light chain/PIN, *Cell Motil. Cytoskeleton* 47 (2000) 269–281.
- [13] J.A. Spudich, S. Watt, The regulation of rabbit skeletal muscle contraction. I. Biochemical studies of the interaction of the tropomyosin-troponin complex with actin and the proteolytic fragments of myosin, *J. Biol. Chem.* 246 (1971) 4866–4871.
- [14] Y.H. Chien, I.B. Dawid, Isolation and characterization of calmodulin genes from *Xenopus laevis*, *Mol. Cell. Biol.* 4 (1984) 507–513.
- [15] S. Maruta, T. Ohki, T. Kambara, M. Ikebe, Characterization of the interaction of myosin with ATP analogues having the syn conformation with respect to the adenine-ribose bond, *Eur. J. Biochem.* 256 (1998) 229–237.
- [16] W.F. Stafford 3rd, Boundary analysis in sedimentation transport experiments: a procedure for obtaining sedimentation coefficient distributions using the time derivative of the concentration profile, *Anal. Biochem.* 203 (1992) 295–301.
- [17] J.S. Philo, A method for directly fitting the time derivative of sedimentation velocity data and an alternative algorithm for calculating sedimentation coefficient distribution functions, *Anal. Biochem.* 279 (2000) 151–163.
- [18] K. Mabuchi, Melting of myosin and tropomyosin: electron microscopic observations, *J. Struct. Biol.* 103 (1990) 249–256.
- [19] K. Mabuchi, Heavy-meromyosin-decorated actin filaments: a simple method to preserve actin filaments for rotary shadowing, *J. Struct. Biol.* 107 (1991) 22–28.
- [20] A.A. Nascimento, R.E. Cheney, S.B. Tauhata, R.E. Larson, M.S. Mooseker, Enzymatic characterization and functional domain mapping of brain myosin-V, *J. Biol. Chem.* 271 (1996) 17561–17569.
- [21] H. Suzuki, H. Onishi, K. Takahashi, S. Watanabe, Structure and function of chicken gizzard myosin, *J. Biochem.* 84 (1978) 1529–1542.
- [22] H. Onishi, T. Wakabayashi, Electron microscopic studies of myosin molecules from chicken gizzard muscle I: the formation of the intramolecular loop in the myosin tail, *J. Biochem.* 92 (1982) 871–879.
- [23] R. Craig, R. Smith, J. Kendrick-Jones, Light-chain phosphorylation controls the conformation of vertebrate non-muscle and smooth muscle myosin molecules, *Nature* 302 (1983) 436–439.
- [24] M. Ikebe, S. Hinkins, D.J. Hartshorne, Correlation of enzymatic properties and conformation of smooth muscle myosin, *Biochemistry* 22 (1983) 4580–4587.
- [25] K.M. Trybus, T.W. Huiatt, S. Lowey, A bent monomeric conformation of myosin from smooth muscle, *Proc. Natl. Acad. Sci. USA* 79 (1982) 6151–6155.
- [26] H. Onishi, T. Wakabayashi, T. Kamata, S. Watanabe, Electron microscopic studies of myosin molecules from chicken gizzard muscle II: the effect of thiophosphorylation of the 20-kdalton light chain on the ATP-induced change in the conformation of myosin monomers, *J. Biochem.* 94 (1983) 1147–1154.
- [27] K.J. Verhey, T.A. Rapoport, Kinesin carries the signal, *Trends Biochem. Sci.* 26 (2001) 545–550.
- [28] M.F. Stock, J. Guerrero, B. Cobb, C.T. Eggers, T.G. Huang, X. Li, D.D. Hackney, Formation of the compact conformation of kinesin requires a COOH-terminal heavy chain domain and inhibits microtubule-stimulated ATPase activity, *J. Biol. Chem.* 274 (1999) 14617–14623.
- [29] D.L. Coy, W.O. Hancock, M. Wagenbach, J. Howard, Kinesin's tail domain is an inhibitory regulator of the motor domain [comment], *Nat. Cell Biol.* 1 (1999) 288–292.
- [30] A.D. Mehta, R.S. Rock, M. Rief, J.A. Spudich, M.S. Mooseker, R.E. Cheney, Myosin-V is a processive actin-based motor, *Nature* 400 (1999) 590–593.
- [31] T. Sakamoto, I. Amitani, E. Yokota, T. Ando, Direct observation of processive movement by individual myosin V molecules, *Biochem. Biophys. Res. Commun.* 272 (2000) 586–590.
- [32] F. Wang, K. Thirumurugan, W.F. Stafford, J.A. Hammer, P.J. Knight, J.R. Sellers, Regulated conformation of myosin V, *J. Biol. Chem.* (2004) in press.